Nearly Blinking-Free, High-Purity Single-Photon Emission by Colloidal InP/ZnSe Quantum Dots

Vigneshwaran Chandrasekaran, Mickaël D. Tessier, Dorian Dupont, Pieter Geiregat, Zeger Hens, and Edouard Brainis*

Center for Nano and Biophotonics and Physics and Chemistry of Nanostructures, Ghent University, Ghent 9000, Belgium

S *Supporting Information*

ABSTRACT: Colloidal core/shell InP/ZnSe quantum dots (QDs), recently produced using an improved synthesis method, have a great potential in life-science applications as well as in integrated quantum photonics and quantum information processing as single-photon emitters. Single-particle spectroscopy of 10 nm QDs with 3.2 nm cores reveals strong photon antibunching attributed to fast (70 ps) Auger recombination of multiple excitons. The QDs exhibit very good photostability under strong optical excitation. We demonstrate that the antibunching is preserved when the QDs are excited above the saturation intensity of the fundamental-exciton transition. This result paves the way toward their usage as high-purity on-demand single-photon emitters at room temperature. Unconventionally, despite the strong Auger blockade mechanism, InP/ZnSe QDs also display very little luminescence intermittency ("blinking"), with a simple on/off blinking pattern. The analysis of single-particle luminescence statistics places these InP/ZnSe QDs in the class of nearly blinking-free QDs, with emission stability comparable to state-of-the-art thick-shell and alloyed-interface CdSe/CdS, but with improved single-photon purity.

KEYWORDS: *Colloidal quantum dots, single-particle, spectroscopy, single-photon emission, blinking*
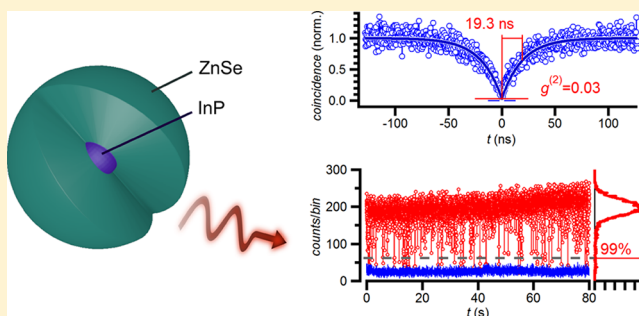
Solid-state emitters providing single photons on-demand are an essential building blocks in photonic quantum technology,[1] which involves applications such as quantum cryptography,[2,3] quantum simulation,[4,5] and quantum metrology.[6] Currently, a diversity of material platforms is considered as single-photon emitters, which include color centers or defects in crystalline hosts,[7−9] carbon nanotubes,[10] transition metal dichalcogenides,[11] and epitaxial[12−14] and colloidal[15−18] semiconductor nanocrystals or quantum dots (QDs). Among these, colloidal QDs stand out since they offer an extensive design freedom (both at the level of nanocrystal synthesis and device integration) as well as room-temperature operation.[12] The emission wavelength of colloidal QDs can be readily tuned by changing their diameter, and they can be formed from several semiconductors. Moreover, colloidal synthesis methods offer an extensive control over the QD size and shape and enable complex heterostructures to be formed. In addition, the resulting QD dispersion or inks can be readily combined with a multitude of technology platforms for further processing.

Room-temperature photon antibunching in the luminescence of single colloidal QDs was first reported for CdSe/ZnS core/shell QDs and attributed to the highly efficient, nonradiative Auger recombination of multiexcitons.[19,20] This enabled the emission of a single photon to be triggered by a high-intensity excitation pulse, with a near-unity probability of photo-excitation and a high-purity single photon emission.[15,16]

However, the further development of CdSe/ZnS QDs as single photon emitters stalled because of their intermittent fluorescence or blinking, which leads to an unpredictable succession of bright and dark periods.[15,20,21] In the case of CdSe/CdS core/shell QDs, it was shown that blinking can be suppressed by implementing sufficiently thick CdS shells.[22,23] However, this approach leads to a significant reduction of the Auger recombination rate, possibly linked to the formation of alloyed interfaces. The concomitant promotion of the radiative recombination of multiexcitons reduces photon antibunching, an effect that is the more pronounced with the higher the biexciton photoluminescence quantum yield.[24] The same issue is faced by attempts to suppress blinking by speeding up radiative recombination through, for example, plasmonic effects.[25] Since accelerating radiative recombination shifts the balance between radiative and nonradiative Auger recombination of multiexcitons, blinking suppression by enhancing radiative recombination also results in a loss of purity of single photon emission.[26]

Currently, the focus of QD synthesis research is shifting to materials made from semiconductors that offer even better optical properties, such as cesium lead halide perovskites
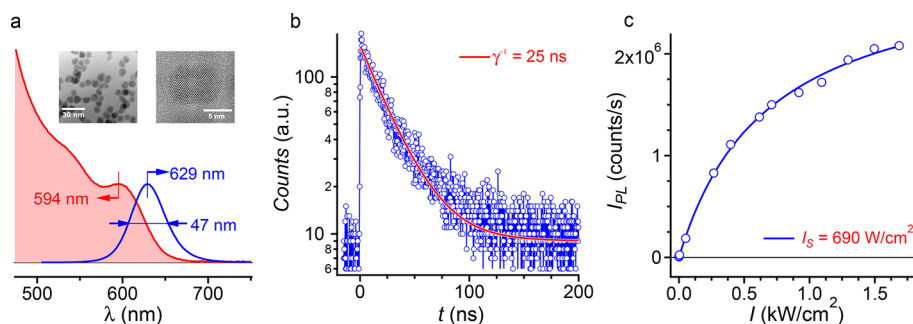
Figure 1. (a) Absorption (red) and emission (blue) spectrum of InP/ZnSe QDs in solution. Insets: TEM and HR-TEM image of the InP/ZnSe QDs. (b) Luminescence decay from InP/ZnSe QDs in a thin film after pulsed excitation at 445 nm. (c) Luminescence saturation under high intensity cw excitation at 445 nm.
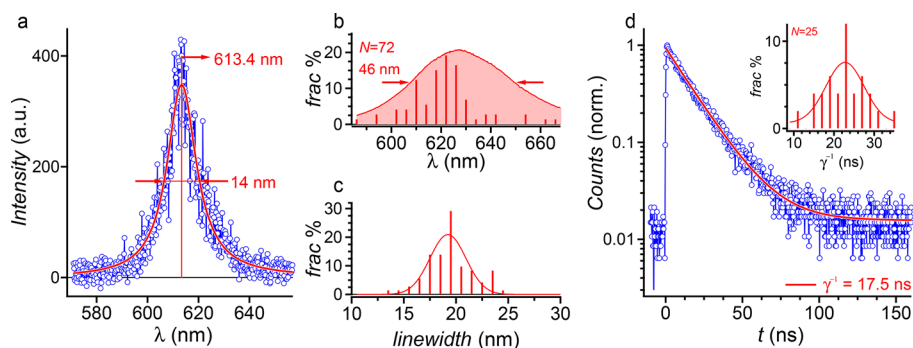

Figure 2. (a) Emission spectrum of a single QD fitted to a Lorentzian function. (b) Statistical distribution of the central emission wavelength in an ensemble of 72 single QDs. (c) Statistical distribution of emission line width for the same ensemble. (d) Luminescence decay trace of a single QD fitted to a single exponential function with a decay time of 17.5 ns. Inset: statistical distribution of the decay times based on an ensemble of 25 single QDs.

(CsPbX$_3$, X = Cl,Br,I), or have a composition nonrestricted by the toxicity regulations on heavy-metal ions in electronic and electro-optical devices, of which InP QDs are the most notable example. Rapidly after the first reports on their synthesis,[27] single CsPbBr$_3$ nanocrystals were shown to exhibit photon antibunching and, in one study, reduced blinking.[28,29] However, as these nanocrystals showed significant photodegradation, it remains unclear whether CsPbBr$_3$ nanocrystals can provide single photons on demand. Opposite from CsPbBr$_3$ nanocrystals, InP QDs received little attention, if any, as possible single-photon emitters even if the first syntheses were developed shortly after the first hot injection synthesis of CdSe QDs.[30] More recently, a new approach to form InP-based QDs has been introduced, based on aminophosphines as the phosphorus precursor.[31,32] This method enables a variety of InP-based core/shell QDs to be formed with widely tunable optical properties. In this respect, the InP/ZnSe core/shell combination is interesting. It features a similar, straddling band alignment as CdSe/ZnS, yet the InP/ZnSe lattice mismatch amounts to a mere 3%, in stark contrast to the 12% mismatch between CdSe and ZnS. Although the atomistic origin of blinking in QDs is still debated,[33] the low-strain, type 1 combination offered by the InP/ZnSe core/shell system could offer a pathway to reconcile nonblinking characteristics with single-photon emission by colloidal QDs.

Here, we study the luminescence of individual InP/ZnSe core/shell QDs (with 3.2 nm cores) synthesized using tris-diethylaminophosphine as the phosphorus precursor according to a recently published procedure (see Supporting Information S1 for details).[34] As shown in Figure 1a, the resulting InP/ZnSe

QDs had an equivalent diameter of about 10 nm (see the inset), and their absorption spectrum exhibited the typical band-edge transition with a maximum at 594 nm. The crystallinity of the particles is evident from the HR-TEM image shown in the inset of Figure 1a. The photoluminescence (PL) in solution featured a concomitant single-peak spectrum around 629 nm, a full width at half-maximum (fwhm) of 47 nm, and a PL quantum yield of 65%. As shown before, this relatively large fwhm (Cd-based QDs, CsPbBr$_3$ or CdSe nanoplatelets can have an ensemble emission as narrow as 20, 12, and 10 nm, respectively) is not a characteristic of the emission of individual InP QDs, yet reflects heterogeneous broadening related to size dispersion.[27,35−37]

We further characterized the PL of the InP/ZnSe QDs by analyzing films spin-coated on a glass coverslip using the microphotoluminescence (μ-PL) setup described in Supporting Information S2. Focusing on ensemble measurements first, Figure 1b represents the PL decay obtained after pulsed excitation at 445 nm. The figure includes a best fit of the experimental data to a single exponential function, $I_{PL}(t) \propto \exp(-\gamma t)$, which yields a PL decay time γ^{-1} = 25 ns. Most interestingly, under continuous wave (cw) excitation at 445 nm, the PL intensity I_{PL} first increases with the excitation intensity I, then saturates according to $I_{PL} \propto I/(I + I_S)$ as expected for an effective two-level transition (see Figure 1c). The fitting of the PL intensity yields a saturation intensity I_S = 690 ± 40 W/cm^2. In combination with the photon energy of the cw excitation laser ($\hbar\omega_p$) and the measured decay rate (γ), this translates into an average QD absorption cross section $\sigma = \hbar\omega_p\gamma/I_S$ of 2.0 ± 0.1 × 10^{-14} cm^2. Using the bulk optical constants of InP and

ZnSe and the dimensions of the core/shell QDs, the absorption cross section of the InP/ZnSe QDs suspended in toluene can be estimated at 2.53×10^{-14} cm^2 (see Supporting Information S3). The correspondence between both figures indicates that the saturation of the PL reflects the emission saturation of the InP/ZnSe QDs and that they behave as effective two-level systems.

To address the PL of single InP/ZnSe QDs, a 1 nM solution of QDs in toluene was dropcast on a glass coverslip, producing a QD surface density of 0.25 μm^{-2}. Figure 2a shows that a single InP/ZnSe QD features a much more narrow emission line than those observed in QD ensembles. A systematic study of 72 single InP/ZnSe QDs showed similarly narrow lines falling within the ensemble emission spectrum (see Figure 2b), confirming that the ensemble emission is heterogeneously broadened. The line widths of single-QD emissions also show some variability (see Figure 2c). While the average fwhm amounts to 19.4 nm, the distribution shows a standard deviation of 2.5 nm and the measured values range from 13 to 24 nm. Finally, we found that single InP/ZnSe QDs exhibit a single-exponential PL decay (see Figure 2d). By investigating an ensemble of 25 QDs, it turned out that the distribution of the decay times γ^{-1} can be fitted to a normal law with an average value of 22.5 ns and a standard deviation of 5.4 ns (see inset to Figure 2d). Similar variations in single QD lifetime have been reported before in the case of CdSe/ZnS QDs.[38] We found that the emission lifetime of each QD is strongly correlated to the central energy $E = hc/\lambda$ of the emitted photons; no discernible correlation between the spectral line width and the photon energy was noticed (see Supporting Information S4).

Strong photon antibunching was observed from single InP/ZnSe QDs. Figure 3a shows the second-order correlation function $g^{(2)}(t)$ of a single QD measured under cw-laser
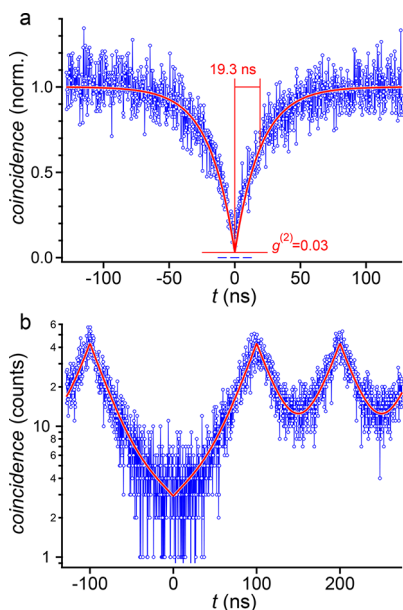
pumping at 445 nm. The antibunching in Figure 3a is almost ideal with only a residual background-limited zero-delay value $g^{(2)}(0) = 0.03$. We fitted the data to the function $g^{(2)}(t) = 1 - [1 - g^{(2)}(0)] \exp(-(\gamma + w_p)|t|)$, where $w_p = \sigma I/(\hbar \omega_p)$ is the pumping rate of the QD and γ its luminescence decay rate.[39] The experiment was performed in a weak excitation regime ($w_p \ll \gamma$). The fit yields $(\gamma + w_p)^{-1} \approx \gamma^{-1} = 19.3$ ns in line with the luminescence decay time statistics measured by direct photon timing (see previous paragraph). We also excited the same QD with 445 nm picosecond pulses at a repetition rate of 10 MHz. No zero-delay peak was seen in the second-order correlation function (see Figure 3b), even in logarithmic scale, confirming that multiexciton emission is very efficiently quenched by nonradiative recombination of charge carriers. We measured the $g^{(2)}(0)$ value of 70 single QDs in the cw-pumping regime and found a mean value of 0.19 with a standard deviation of 0.1 (see Supporting Information S5). In each case, the antibunching was limited by the residual background noise, not by multiexciton emission.

A high photoluminescence quantum yield (PLQY) and strong antibunching are key for using InP/ZnSe QDs as integrated single-photon emitters in quantum technology applications. In this perspective, it is crucially important that antibunching be preserved in the saturation regime when $I \gg I_S$ (equivalently, $w_p \gg \gamma$), such that $I/(I + I_S) = w_p/(w_p + \gamma) \approx 1$. If this condition is fulfilled, the emitter can act as a photon gun, i.e, a short-pulse excitation with sufficient fluence can completely invert the population of the effective two-level system and trigger the spontaneous emission of a single photon with a probability equal to the PLQY. In Figure 4a, we
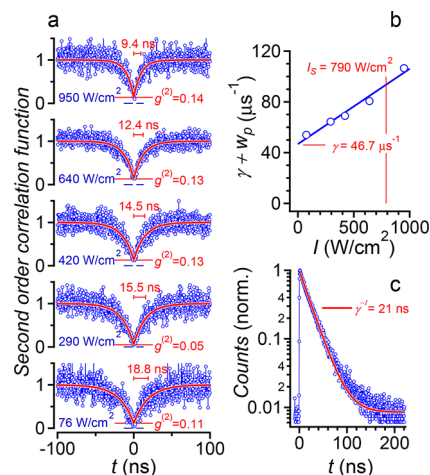
Figure 4. (a) Second-order correlation function of a single QD at different cw-pumping intensities at 445 nm. (b) Antibunching width-constant $\gamma + w_p$ as a function of the pump intensity. (c) Luminescence decay of the QD as a function of time.

Figure 3. (a) Second-order correlation function $g^{(2)}(t)$ of a QD under cw excitation at 445 nm. (b) Second-order correlation function of the same QD under 445 nm (picosecond) pulse excitation at a repetition rate of 10 MHz. The strong antibunching is raw data, without background subtraction nor compensation for intensity differences in start/stop channels.

therefore show second-order correlation traces recorded on a single InP/ZnSe QD at pump intensities increasing from 76 to 950 W/cm^2. Over the entire intensity range, the luminescence of the QD preserved a strong antibunching, with a narrowing of the zero-delay dip at higher pump intensity and a stable background-noise limited $g^{(2)}(0)$ between 0.05 and 0.14. By fitting the $g^{(2)}$ functions, we could determine the time constant $(\gamma + w_p)^{-1}$ as indicated in Figure 4a. It can be seen that this time constant is always smaller than the emission lifetime, determined at $\gamma^{-1} = 21$ ns for this particular QD (see Figure

4c), and drops from 18.8 to 9.4 ns with increasing pump intensity.

Figure 4b represents $\gamma + w_p$ as a function of the pump intensity I. In line with the linear dependence of w_p on the pump intensity, $\gamma + w_p$ changes linearly with I. A best fit yields a slope $\sigma/(\hbar\omega_p)$ of 5.9×10^4 cm^2/J, from which we obtain the absorption cross-section of the QD as $\sigma = 2.0 \times 10^{-14}$ cm^2. This figure is equal to the ensemble value that was derived from the photoluminescence saturation as plotted in Figure 1c. By extrapolating the data in Figure 4b to the $I \rightarrow 0$ limit, we find the luminescence decay rate of the QD as $\gamma = 46.7$ μs^{-1}, a figure that agrees well with the luminescence decay time $\gamma^{-1} = 21$ ns obtained in a direct photon-timing experiment (see Figure 4c). By combining σ and γ, we obtain the saturation intensity of the QD as $I_S = \hbar\omega_p\gamma/\sigma = 790$ W/cm^2. Hence, the data shown in Figure 4 demonstrate that strong antibunching is preserved for pumping intensities up to $1.2 \times I_S$, with no sign of multiexciton emission nor significant photodegradation of the emitter, two essential properties enabling the use of InP/ZnSe QDs as triggered single-photon emitters in quantum optics applications.

In the case of CdSe/ZnS, the persistence of photon antibunching when pumping single QDs above the saturation intensity was attributed to the quenching of radiative recombination of multiexcitons by fast Auger recombination.[20] To quantify the rate of Auger recombination, and thus the yield of multiexciton emission in the case of the InP/ZnSe QDs studied here, we analyzed the transient absorbance of an InP/ZnSe dispersion after femtosecond optical pumping. As discussed in the Supporting Information S6, an additional decay component with a time constant of $\sim$70 ps appeared in the transient absorption at high pump intensities. Such a fast component is a typical characteristic of Auger recombination of multiexcitons.[40] We therefore interpret the corresponding decay rate $\gamma_{XX} = 14.3$ ns^{-1} as the combined result of biexciton decay by radiative and nonradiative (Auger) recombination, i.e., $\gamma_{XX} = \gamma_{r,XX} + \gamma_{nr,XX}$. Writing the radiative recombination rate of biexcitons[41] as $\gamma_{r,XX} = 4\gamma$ ($\gamma^{-1} = 36$ ns is the decay time of the fundamental exciton in solution), we can estimate the radiative biexciton quantum yield in InP/ZnSe QDs as $PLQY_{XX} = \gamma_{r,XX}/\gamma_{XX} = 0.77\%$. This very low value explains why single-photon emission is retained at high pumping power.

Our InP/ZnSe QDs are subject to some modest fluorescence intermittency, a phenomenon commonly known as "blinking". At the ensemble level, blinking merely reduces the effective PLQY of the material. In quantum optics applications, however, blinking prohibits the use of single QDs as deterministic single-photon turnstile devices. The data in Figure 5a (red line) show the intensity of the light (photon counts per 10 ms time bin) collected from the QD in Figure 4 as a function of time. The QD was excited with a cw 445 nm laser beam in the low-pumping regime ($I \ll I_S$). The noise background of the measurement is shown in blue. Although some dark periods (no emission, off state) can be seen, the histogram of counts displayed on the right of Figure 5a indicates that 99% of time the QD is bright (on state) and emits photons at a stable rate. The threshold between on and off states is indicated by the dashed gray line in Figure 5a. It was chosen as 2−3 standard deviations above the background noise level as can be seen in Figure 5a. The blinking is very limited and follows a simple on/off pattern, without any intermediate or gray-state emission, as often reported in the case of CdSe/CdS QDs.[42] We studied the blinking of 25 different QDs and observed each time the same
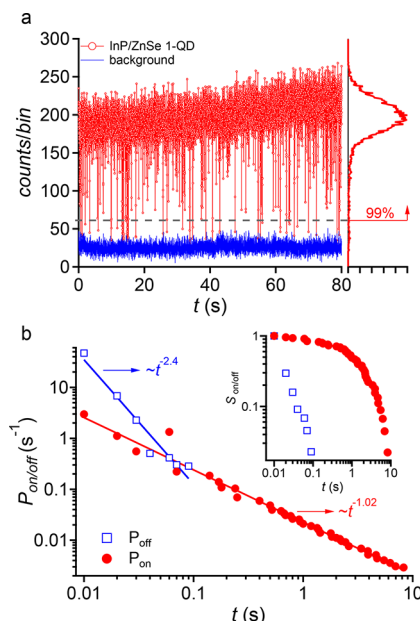

Figure 5. (a) Luminescence intensity of the QD in Figure 4 as a function of time (in counts per 10 ms time bin). The QD is excited with cw 445 nm laser light. (b) Probability density distributions of the on and off time periods. The data is fitted to power law distributions $P_{on(off)}(t) \propto t^{-k_{on(off)}}$ with $k_{off} = 2.44$ and $k_{on} = 1.02$. Inset: survival probabilities $S_{on(off)}(t) = \int_t^\infty P_{on(off)}(\tau)\, d\tau$ constructed from the data in panel b.

two-state (on/off) pattern, with a on-state fraction of 95.5% on average.

To benchmark the fluorescence intermittency in the InP/ZnSe QDs studied here against the extensively studied CdSe/CdS QDs, we define the probability density distributions $P_{on}(t)$ and $P_{off}(t)$ for the QD to stay in an on or an off state during the time t. The shortest on or off duration is determined by the selected binning time, which is 10 ms in our measurements, and the longest duration is limited by the emission characteristics of the QD and the time duration of the measurement. The two distributions are calculated from the data in Figure 5a in the following way:

$$P_{on(off)}(t_n) = \frac{\text{number of "on" ("off") events of duration } t_n}{\text{total number of "on" ("off") events}}$$
$$\times \frac{1}{\Delta_{avg}(t_n)} \tag{1}$$

Here, $\Delta_{avg}(t_n) = (t_{n+1} - t_{n-1})/2$ is the average of the time intervals to the next shorter and next longer observed events.[43] The distributions $P_{on}(t)$ (red dots) and $P_{off}(t)$ (blue open squares) are plotted in Figure 5b in a log−log scale. The linear alignment of the data points in Figure 5b indicates that both $P_{on}(t)$ and $P_{off}(t)$ follow an inverse power law: $P_{on(off)}(t) \propto t^{-k_{on(off)}}$ and linear regression (plain lines in Figure 5b) show that $k_{off} = 2.44$ and $k_{on} = 1.02$. The steeper slope of the off events makes off periods of 10 ms about 100 times more likely than 100 ms ones. A similar analysis was performed on 25 different QDs. We found an average value of 1.2 for k_{on} and 2.2 for k_{off}. A value of $k_{off} > 2$ is indicative of efficient blinking suppression and comparable to the values reported in a nearly blinking-free CdSe/CdS QD.[36,44] In the inset of Figure 5b, we display the survival probabilities $S_{on(off)}(t) = \int_t^\infty P_{on(off)}(\tau)\, d\tau$, which represent the probability to find the QD in an on or an off state

for a time longer than t. Given the power-law distribution of $P_{on}(t)$ and $P_{off}(t)$, the survival probabilities $S_{on(off)}(t)$ scale in principle as $t^{-(k_{on(off)}-1)}$. However, as $k_{on} \approx 1$, $S_{on}(t)$ departs from this power law. The survival probabilities show even more clearly that the off periods are remarkably short (10−100 ms), while the on periods often last a few seconds or more. As can be seen in the inset of Figure 5b, the probability that a QD turns on to remain bright during more than one second is about 50%. Such long on periods are comparable to those reported by Mahler et al. in their study on thick-shell nonblinking CdSe/CdS QDs.[23] This observation puts the InP/ZnSe QDs studied here among today's state-of-the-art nearly blinking-free quantum dots.

For a different QD, we analyzed the blinking behavior at excitation intensities up to ten times higher than in the low-pumping regime discussed above (see Supporting Information S7). As we increase the excitation intensity, we observe a slight increase of the k_{on} values and a slight decrease of the k_{off} values. Even at excitation intensities close to saturation, the off states of the QD are still much shorter than the on states. The plot of the survival probabilities confirms that the QD remains predominantly in an on state. The stable emission in addition to the preserved antibunching at saturation intensities further consolidates our point that this type of InP/ZnSe QD is suitable for applications in quantum optics.

In conclusion, we have characterized single InP/ZnSe colloidal QDs showing a unique combination of narrow room-temperature emission spectrum, strong antibunching, monoexponential luminescence decay, reduced blinking, and photostability. Our single particle spectroscopy study demonstrates that single-photon emission is preserved at saturating intensities, which we attribute to fast nonradiative Auger recombination of multiexcitons. Although these fast multiexciton recombination rates might limit their use for light amplification, these QDs are ideally suited for quantum optics applications as single-photon turnstile devices. Furthermore, reduced cytotoxicity offers them a prospect in life-science applications. There is scope for further improving the synthesis of the QDs toward even better optical properties. This opens perspectives for future comparative analyses of InP dots with different core/shell sizes, different shell materials, studies at cryogenic temperatures, and suitability for nanolithographic deposition.

ASSOCIATED CONTENT

ⓢ Supporting Information

The Supporting Information is available free of charge on the ACS Publications website at DOI: 10.1021/acs.nanolett.7b02634.

> Materials and chemical synthesis. Microphotoluminescence setup. Theoretical calculation of absorption cross section. Correlation between emission lifetime, line width, and central energy. QD antibunching: $g^{(2)}(0)$ statistics. Pump−probe measurements. Excitation-intensity dependence of blinking statistics (PDF)

AUTHOR INFORMATION

Corresponding Author

*E-mail: edouard.brainis@ugent.be. Phone: +32-9-2644418.

ORCID Ⓘ

Zeger Hens: 0000-0002-7041-3375
Edouard Brainis: 0000-0003-4720-1793

REFERENCES

(1) Aharonovich, I.; Englund, D.; Toth, M. Nat. Photonics 2016, 10, 631−641.
(2) Beveratos, A.; Brouri, R.; Gacoin, T.; Villing, A.; Poizat, J.-P.; Grangier, P. Phys. Rev. Lett. 2002, 89, 187901.
(3) Heindel, T. New J. Phys. 2012, 14, 083001.
(4) Broome, M. A.; Fedrizzi, A.; Lanyon, B. P.; Kassal, I.; Aspuru-Guzik, A.; White, A. G. Phys. Rev. Lett. 2010, 104, 153602.
(5) Tillmann, M.; Dakić, B.; Heilmann, R.; Nolte, S.; Szameit, A.; Walther, P. Nat. Photonics 2013, 7, 540−544.
(6) Motes, K. R.; Olson, J. P.; Rabeaux, E. J.; Dowling, J. P.; Olson, S. J.; Rohde, P. P. Phys. Rev. Lett. 2015, 114, 170802.
(7) Aharonovich, I.; Neu, E. Adv. Opt. Mater. 2014, 2, 911−928.
(8) Morfa, A. J.; Gibson, B. C.; Karg, M.; Karle, T. J.; Greentree, A. D.; Mulvaney, P.; Tomljenovic-Hanic, S. Nano Lett. 2012, 12, 949−954.
(9) Utikal, T.; Eichhammer, E.; Petersen, L.; Renn, A.; Götzinger, S.; Sandoghdar, V. Nat. Commun. 2014, 5, 3627.
(10) Ma, X.; Hartmann, N. F.; Baldwin, J. K.; Doorn, S. K.; Htoon, H. Nat. Nanotechnol. 2015, 10, 671−675.
(11) He, Y.-M.; Clark, G.; Schaibley, J. R.; He, Y.; Chen, M.-C.; Wei, Y.-J.; Ding, X.; Zhang, Q.; Yao, W.; Xu, X.; Lu, C.-Y.; Pan, J.-W. Nat. Nanotechnol. 2015, 10, 497−502.
(12) Buckley, S.; Rivoire, K.; Vučković, J. Rep. Prog. Phys. 2012, 75, 126503.
(13) Patel, R. B.; Bennett, A. J.; Farrer, I.; Nicoll, C. A.; Ritchie, D. A.; Shields, A. J. Nat. Photonics 2010, 4, 632−635.
(14) Sapienza, L.; Davanço, M.; Badolato, A.; Srinivasan, K. Nat. Commun. 2015, 6, 7833.
(15) Brokmann, X.; Giacobino, E.; Dahan, M.; Hermier, J.-P. Appl. Phys. Lett. 2004, 85, 712−714.
(16) Brokmann, X.; Messin, G.; Desbiolles, P.; Giacobino, E.; Dahan, M.; Hermier, J.-P. New J. Phys. 2004, 6, 99.
(17) Pisanello, F.; Martiradonna, L.; Leménager, G.; Spinicelli, P.; Fiore, A.; Manna, L.; Hermier, J.-P.; Cingolani, R.; Giacobino, E.; De Vittorio, M.; Bramati, A. Appl. Phys. Lett. 2010, 96, 033101.
(18) Pisanello, F.; Leménager, G.; Martiradonna, L.; Carbone, L.; Vezzoli, S.; Desfonds, P.; Cozzoli, P. D.; Hermier, J.-P.; Giacobino, E.; Cingolani, R.; De Vittorio, M.; Bramati, A. Adv. Mater. 2013, 25, 1974−1980.
(19) Michler, P.; Imamoglu, A.; Mason, M. D.; Carson, P. J.; Strouse, G. F.; Buratto, S. K. Nature 2000, 406, 968−970.
(20) Lounis, B.; Bechtel, H. A.; Gerion, D.; Alivisatos, P.; Moerner, W. E. Chem. Phys. Lett. 2000, 329, 399−404.
(21) Nirmal, M.; Dabbousi, B. O.; Bawendi, M. G.; Macklin, J. J.; Trautman, J. K.; Harris, T. D.; Brus, L. E. Nature 1996, 383, 802−804.
(22) Chen, Y.; Vela, J.; Htoon, H.; Casson, J. L.; Werder, D. J.; Bussian, D. A.; Klimov, V. I.; Hollingsworth, J. A. J. Am. Chem. Soc. 2008, 130, 5026−5027.
(23) Mahler, B.; Spinicelli, P.; Buil, S.; Quelin, X.; Hermier, J.-P.; Dubertret, B. Nat. Mater. 2008, 7, 659−664.
(24) Park, Y.-S.; Bae, W. K.; Padilha, L. A.; Pietryga, J. M.; Klimov, V. I. Nano Lett. 2014, 14, 396−402.
(25) Yuan, C. T.; Yu, P.; Ko, H. C.; Huang, J.; Tang, J. ACS Nano 2009, 3, 3051−3056.

(26) Naiki, H.; Masuo, S.; Machida, S.; Itaya, A. *J. Phys. Chem. C* **2011**, *115*, 23299−23304.

(27) Protesescu, L.; Yakunin, S.; Bodnarchuk, M. I.; Krieg, F.; Caputo, R.; Hendon, C. H.; Yang, R. X.; Walsh, A.; Kovalenko, M. V. *Nano Lett.* **2015**, *15*, 3692−3696.

(28) Park, Y.-S.; Guo, S.; Makarov, N. S.; Klimov, V. I. *ACS Nano* **2015**, *9*, 10386−10393.

(29) Raino, G.; Nedelcu, G.; Protesescu, L.; Bodnarchuk, M. I.; Kovalenko, M. V.; Mahrt, R. F.; Stoeferle, T. *ACS Nano* **2016**, *10*, 2485−2490.

(30) Micic, O. I.; Curtis, C. J.; Jones, K. M.; Sprague, J. R.; Nozik, A. J. *J. Phys. Chem.* **1994**, *98*, 4966−4969.

(31) Song, W.-S.; Lee, H.-S.; Lee, J. C.; Jang, D. S.; Choi, Y.; Choi, M.; Yang, H. *J. Nanopart. Res.* **2013**, *15*, 1750.

(32) Tessier, M. D.; Dupont, D.; De Nolf, K.; De Roo, J.; Hens, Z. *Chem. Mater.* **2015**, *27*, 4893−4898.

(33) Efros, A. L.; Nesbitt, D. J. *Nat. Nanotechnol.* **2016**, *11*, 661−671.

(34) Tessier, M. D.; De Nolf, K.; Dupont, D.; Sinnaeve, D.; De Roo, J.; Hens, Z. *J. Am. Chem. Soc.* **2016**, *138*, 5923−5929.

(35) Ithurria, S.; Tessier, M. D.; Mahler, B.; Lobo, R. P. S. M.; Dubertret, B.; Efros, A. L. *Nat. Mater.* **2011**, *10*, 936−941.

(36) Chen, O.; Zhao, J.; Chauhan, V. P.; Cui, J.; Wong, C.; Harris, D. K.; Wei, H.; Han, H.-S.; Fukumura, D.; Jain, R. K.; Bawendi, M. G. *Nat. Mater.* **2013**, *12*, 445−451.

(37) Cui, J.; Beyler, A. P.; Marshall, L. F.; Chen, O.; Harris, D. K.; Wanger, D. D.; Brokmann, X.; Bawendi, M. G. *Nat. Chem.* **2013**, *5*, 602−606.

(38) Fisher, B. R.; Eisler, H. J.; Stott, N. E.; Bawendi, M. G. *J. Phys. Chem. B* **2004**, *108*, 143−148.

(39) Michler, P. In *Single Quantum Dots: Fundamentals, Applications, and New Concepts*; Michler, P., Ed.; Springer Berlin Heidelberg: Berlin, Heidelberg, 2003; Chapter 8, pp 315−347.

(40) Klimov, V. I.; Mikhailovsky, A. A.; McBranch, D. W.; Leatherdale, C. A.; Bawendi, M. G. *Science* **2000**, *287*, 1011−1013.

(41) Garcia-Santamaria, F.; Brovelli, S.; Viswanatha, R.; Hollingsworth, J. A.; Htoon, H.; Crooker, S. A.; Klimov, V. I. *Nano Lett.* **2011**, *11*, 687−693.

(42) Spinicelli, P.; Buil, S.; Quélin, X.; Mahler, B.; Dubertret, B.; Hermier, J.-P. *Phys. Rev. Lett.* **2009**, *102*, 136801.

(43) Kuno, M.; Fromm, D. P.; Hamann, H. F.; Gallagher, A.; Nesbitt, D. J. *J. Chem. Phys.* **2001**, *115*, 1028−1040.

(44) Hohng, S.; Ha, T. *J. Am. Chem. Soc.* **2004**, *126*, 1324−1325.